Science and Technology Indonesia
e-ISSN:2580-4391 *p*-ISSN:2580-4405
Vol. 11, No. 2, April 2026

Research Paper

Utilization of Diatom Frustule Waste from *Navicula* sp. TAD as Photoelectrode Material for Enhancing the Efficiency of Dye-Sensitized Solar Cells (DSSC)

Ivonne Telussa[1*], Hellna Tehubijuluw[1], Eka Rahmat Mahayani Anthonia Putera Lilipaly[2], Dominggus Malle[3], Riona Magdalena Amarduan[1]

[1]*Department of Chemistry, Faculty of Science and Technology, Pattimura University, Poka Campus, Pattimura University, Maluku, 97134, Indonesia*
[2]*Department of Mechanical Engineering, Faculty of Engineering, Ambon Polytechnic, Ambon, Maluku, 97233, Indonesia*
[3]*Department of Animal Husbandry, Faculty of Agriculture, Pattimura University, Poka Campus, Pattimura University, Maluku, 97134, Indonesia*
***Corresponding author**: ivonnetelussa@gmail.com

Abstract
Navicula sp. TAD is a microalga with silica-based cell walls, offering potential to improve photon interaction in dye-sensitized solar cells (DSSCs). This study combined *Navicula* sp. TAD frustules with TiO_2 to fabricate DSSC working electrodes. The objectives were to isolate and characterize the frustules, optimize the TiO_2–frustule ratio, and evaluate photoelectric performance. The workflow consisted of cultivating *Navicula* sp., isolating pigments and frustules, fabricating solar cells with varied electrode compositions, and performing photoelectric testing under a solar simulator. Fourier Transform Infrared Spectroscopy (FTIR), X-Ray Diffraction (XRD), and Scanning Electron Microscope (SEM) analysis confirmed that the frustules possess nanoporous surfaces and exhibit Si–O–Si and Si–OH functional groups. Electrodes incorporating TiO_2–frustule blends showed compact pore networks, along with additional functional groups. Performance screening across compositions identified an optimal TiO_2–frustule ratio of 40:60, which delivered an efficiency of 10.51%, a short-circuit current density of 0.673 A, an open-circuit voltage of 301.8 mV, and a fill factor of 0.32. These findings indicate that frustule-enabled light management and surface chemistry can jointly enhance dye loading and charge collection in DSSC photoanodes relative to TiO_2 alone.

Keywords
Diatom, Frustule Waste, Dye-Sensitized Solar Cells (DSSC), *Navicula* sp. TAD, Photoelectrode Material, Solar Cell Efficiency

Received: 30 May 2025, Accepted: 14 February 2026
https://doi.org/10.26554/sti.2026.11.2.632-642

1. INTRODUCTION

Energy is essential for human life. In general, energy sources are divided into two types: renewable and non-renewable. Currently, most countries still rely on fossil fuels such as coal, oil, and natural gas. If continuously consumed, these resources will eventually be depleted. Therefore, transitioning to renewable energy is crucial for long-term sustainability. One promising renewable energy source is solar energy. Indonesia, located in the tropical zone (6° N–11° S), receives abundant sunlight that can be converted into electricity without causing environmental pollution. The technology used for this conversion is photovoltaic solar cells (Wahyudi et al., 2023; Langer et al., 2021).

Solar cell research has advanced rapidly, enhancing both production and utilization as an energy source. Traditional crystalline silicon production, from its early stages to today, continues to face challenges due to the need for high-quality silicon and energy-intensive fabrication processes, resulting in relatively high production costs and a significant environmental footprint during manufacturing. These findings are supported by life-cycle assessment studies that highlight the roles of energy consumption, silicon usage, and the carbon intensity of electricity during production as the main contributors to environmental impact (Latunussa et al., 2016; Müller et al., 2021). To overcome these issues, researchers developed dye-sensitized solar cells (DSSC) using cheaper materials and simpler methods. Invented by Dragonetti, DSSCs use wide-bandgap semiconductor nanocrystals instead of silicon (Dragonetti and Colombo, 2021). Light excites electrons in TiO_2 via dye absorption, generating electricity and regenerating the dye (Kurniawan et al., 2025).

Titanium dioxide (TiO_2) is a semiconductor known for its high photocatalytic activity, stability, and non-toxicity. Commercial TiO_2 powder is widely available and can be mass-produced(Kurniawan et al., 2025). When exposed to UV light ($\leq$ 390 nm), electrons are excited to the conduction band, leaving holes in the valence band (Baig et al., 2025). These holes react with OH^- ions to form hydroxyl radicals ·OH, which break down organic compounds. However, its effectiveness is

limited by electron-hole recombination. Modifying TiO_2 with ZnO, CuO, SiO_2, and Fe_2O_3 enhances performance. Metal doping and sensitization with dyes extend its activity into the visible spectrum, making pollutant degradation more efficient and faster (Sambrano et al., 2003).

Diatom frustules can improve the photoresponse of TiO_2 in dye-sensitized solar cells (DSSC). Diatoms are unicellular microalgae from Bacillariophyceae, found in marine and freshwater environments (Bandara et al., 2020; Huang et al., 2015). They absorb silicate and form silica-based cell walls, making them resistant to environmental stress. Their porous, 3D exoskeleton ranges from 50 nm to over 1 micron, with overall sizes up to 1 mm depending on species (Chen et al., 2015). Diatom frustules enhance light-trapping and scattering (Huang et al., 2015). Frustules contain silica (TiO_2), a *p*-type semiconductor known for its mechanical and thermal stability, inertness, and hydrophilicity. These properties provide a large surface area and porosity, allowing better dye absorption than TiO_2, which can improve DSSC efficiency.

Although biodiesel waste from diatoms in the form of frustules is rarely explored for DSSC electrodes, its silica content offers potential as an optical element. Chen et al. (2015) demonstrated that placing frustules on light-absorbing surfaces significantly enhances visible light absorption. Silica isolation from frustules can be done using strong acids like HCl, resulting in white coloration that indicates organic removal (Telussa et al., 2022). These characteristics make frustules ideal for improving dye absorption in DSSCs (Chen et al., 2015; Wang and Seibert, 2017; De Tommasi et al., 2017; Rogato and De Tommasi, 2020).

Dye-sensitized solar cells (DSSC) are a promising renewable energy technology due to their low cost and ease of fabrication. Previous studies have explored the use of diatom frustules to enhance DSSC performance. Huang et al. (2015) showed that replacing one TiO_2 layer with diatom frustule paste increased power conversion efficiency from 3.81% to 5.26%. Toster et al. (2013) used frustules coated with titania nanoparticles (<20 nm), improving efficiency from 3.5% to 4.6%. Bandara et al. (2020) demonstrated that combining TiO_2 nanocrystals (14 nm) with pennate diatom frustules raised efficiency from 3.04% to 4.65%. These findings highlight the potential of frustules to improve light absorption and scattering. However, research on frustules from *Navicula* sp. a diatom endemic to Ambon Bay Telussa et al. (2021)—remains limited. *Navicula* sp. is abundant, easy to cultivate, and contains silica-based cell walls with carotenoids and chlorophyll a and c pigments (Telussa et al., 2019), making it ideal for DSSC applications. This study investigates the novelty of using *Navicula* sp. frustules as photoelectrode material in DSSCs. It aims to support renewable energy development in remote island regions like Maluku, where DSSCs could offer practical, community-based energy solutions.

2. EXPERIMENTAL SECTION

2.1 Materials

The *Navicula* sp. TAD strain was obtained from the Culture Collection of Algae at the Biochemistry Laboratory, Department of Chemistry, Faculty of Mathematics and Natural Sciences, Pattimura University. All chemicals used in this study were of pro-analysis grade and sourced from Merck, Germany, including ethanol, ethyl acetate, n-hexane, acetone, silica gel, and titanium dioxide (TiO_2) powder. The laboratory equipment utilized included standard glassware, Indium Tin Oxide (ITO)-coated glass slides, an analytical balance (Ohaus Adventurer Pro), a hot plate (Cimarec 2), a Rotary Vacuum Evaporato (BUCHI R-18), and an autoclave (TOMY ES-215). Supporting instruments included a refractometer, micropipettes (100–1000 μL), a hemacytometer, and a centrifuge (Thermo Scientific S16). For advanced analysis, a light microscope (Nikon YS-100), a solar simulator (GUNT HL 313.01), a UV-Vis Spectrophotometer (Shimadzu UV-2450), Fourier Transform Infrared Spectroscopy (FTIR) (ShimadzuIRTracer-100), X-Ray Diffraction (XRD) (D8 ADVANCE ECO, BRUKER), and a Scanning Electron Microscope (SEM) (HITACHI SU350 0) were employed, all of which played a vital role in the experimental and characterization processes.

2.2 Methods

2.2.1 Cultivation of *Navicula* sp. TAD

The cultivation of *Navicula* sp. TAD was carried out in a modified medium. The initial cell density was set at 5×10^5 cells mL^{-1} within a simple photobioreactor, maintained at room temperature under a light intensity of 67.5 μmol m^{-2} s^{-1}. A controlled photoperiod of 12:12 hours (dark:light) was applied, with a salinity level of 28 ppt and a pH range of 8.2–8.5. Aeration was provided through free air bubbles. The growth and morphological characteristics of the cells were monitored using light microscopy.

2.2.2 Biomass Harvesting of *Navicula* sp. TAD

Cultivated *Navicula* sp. TAD cells were harvested using sedimentation and filtration techniques with nylon cloth. The wet biomass was weighed using an analytical balance to determine its mass. Subsequently, the biomass was dried at a cold temperature until fully dehydrated, after which it was weighed again to obtain the final dry biomass weight.

2.2.3 Photosynthetic Pigment Extraction

A total of 1.7 grams of dry biomass was macerated in an ice bath with 20 mL of acetone solvent for five hours. The dark-colored supernatant was collected and concentrated using a vacuum rotary evaporator until no solvent remained. The dried extract was then transferred into a dark bottle for further drying. The supernatant served as the crude pigment extract for analysis. Subsequently, the crude pigment extract was characterized using thin-layer chromatography (TLC) and UV-Vis Spectrophotometer.

2.2.4 Isolation of *Navicula* sp. TAD Frustules from Biodiesel Waste

A total of 2.50 g of *Navicula* sp. TAD frustule waste from biodiesel production was placed into a 250 mL Erlenmeyer flask and mixed with a 20% HCl solution. The mixture was stirred at a speed of 180 rpm at room temperature (approximately 25°C) for 30 minutes. The reaction product was then centrifuged at 4000 rpm for 10 minutes. The resulting sediment was washed with deionized water and subjected to three rounds of centrifugation to remove residual acid. Following the washing process, the sample was dried in an oven at 60°C for 48 hours to eliminate remaining moisture. After acid treatment, the dried frustule sample was further processed in a furnace for 3 hours, with the combustion temperature set at 600°C (Telussa et al., 2022). Frustule characterization was performed using Fourier Transform Infrared Spectroscopy (FTIR), Scanning Electron Microscopy (SEM), and X-ray Diffraction (XRD).

2.2.5 Indium Tin Oxide (ITO) Glass Preparation

Before use, indium tin oxide (ITO) glass was first cleaned with a specialized glass detergent, followed by sequential washing with acetone, deionized water, and ethanol. Once thoroughly cleaned, the ITO glass was sonicated for 20 minutes and then rinsed until it was completely free of contaminants. The glass was then dried in an oven at 60°C, preparing it for further application (Chiba et al., 2006). The substrate used in solar cell fabrication consisted of transparent conductive ITO glass with dimensions of 2.5 × 2.5 cm.

2.2.6 Solar Cell Manufacturing

The fabricated solar cells in this study utilized crude pigment extracts from the photosynthetic *Navicula* sp. strain TAD. The study employed variations of TiO_2-frustule paste in compositions of 100:0, 60:40, and 20:80 % (w/w), which were preprocessed and contained nano-sized semiconductor particles. The solar cell assembly required two main components, structured similarly to a sandwich: the anode and the cathode. In the anode section, the edges of the indium tin oxide (ITO) glass (2.5 × 2.5 cm) were covered with adhesive tape, forming an active surface area of 0.5 × 0.5 cm, which was then coated with the working electrode paste. The paste was applied to the conductive glass using the doctor blade method, where a stirring rod was used to spread the electrode paste evenly. After obtaining a thin film layer, the glass was dried at room temperature, and the adhesive tape was removed from the conductive surface. The coated glass was then heated at 450°C for 30 minutes and cooled to room temperature (Hara and Arakawa, 2003). The prepared working electrode was then treated with a pigment solution, which had been re-dissolved in acetone to enhance the light sensitivity of the active anode surface. For the cathode, ITO glass of identical size and surface area was coated with a carbon layer, derived from candle soot residue. The solar cell device was assembled by sandwiching the anode and cathode together, secured using paper clips. Before sealing, a thin adhesive tape was applied to the conductive glass regions lacking TiO_2 (TiO_2-coated conductive glass) to prevent direct contact with the cathode. An electrolyte solution of KI/I_2 (0.5 M KI/0.05 M I_2 in 25 mL deionized water) was injected into the side gaps of the device. Finally, the working electrode was characterized using Fourier Transform Infrared Spectroscopy (FTIR), Scanning Electron Microscopy (SEM), and X-ray Diffraction (XRD).

2.2.7 Dye-Sensitized Solar Cell (DSSC) Efficiency Measurement

The solar cell's ability to capture light and convert it into electrical current was evaluated. The light source used in the experiment was the Sol 3A solar simulator (AM 1.5) with a power output of 100 mW cm^{-2}, an intensity of 1 Sun (94,000 lux = 1269 μmol m^{-2} s^{-1}), and a 10 cm distance between the light source and the solar cell. The electrical current and voltage generated by the solar cell were measured using an ammeter and a voltmeter. Based on the recorded electrical current at specific voltages, key performance parameters such as Jsc (short-circuit current density), Voc (open-circuit voltage), FF (fill factor), and η (conversion efficiency) were determined (Grätzel, 2003).

3. RESULTS AND DISCUSSION

3.1 Cultivation of *Navicula* sp. TAD

The cultivation of *Navicula* sp. TAD was conducted in 2 L glass bottles, functioning as simple photobioreactors, with an initial cell density of 5 × 10^5 cells/mL. The success of the cultivation process was supported by maintaining optimal conditions within the photobioreactor, which facilitated microalgae growth. These conditions included a light intensity of 5000 lux, a salinity level of 28 ppt, a controlled photoperiod of 12:12 hours (dark:light), free aeration, and a nutrient-rich medium containing nitrate, silicate, iron, and phosphate. The *Navicula* sp. TAD cells were cultivated for nine days, during which noticeable changes in culture color and cell density were observed. A gradual darkening of the culture indicated an increase in cell count and higher biomass productivity (Figure 1a).

Cell morphology observation was conducted using light microscopy. Figure 1b presents an image of the cells observed on day 9, showing that *Navicula* sp. TAD exhibits an elongated shape, resembling the letter "D," and a yellow coloration. The yellow hue in *Navicula* sp. cells indicates a high concentration of carotenoid pigments, which are the dominant pigments in these microalgae (Telussa et al., 2019; Bhardwaj et al., 2025).

3.2 Harvesting of *Navicul*a sp. TAD Biomass

Harvesting can be defined as a process of separating water from the growth medium to enhance biomass productivity. In this study, the harvesting of *Navicula* sp. TAD culture was conducted using sedimentation and filtration techniques (Figures 2a and 2b). Sedimentation is a physical separation method that utilizes the force of gravity to separate particles. The greater the difference in density and particle size, the faster the sedimentation process occurs. Conversely, if the density and particle size differences are minimal, the sedimentation process slows down.

Figure 1. Cultivation of *Navicula* sp. TAD. (a) Culture Color Observed on Days 0, 2, 4, 6, 8, and 9 (From Left to Right), (b) Cell Morphology

Filtration, on the other hand, was performed using nylon cloth to separate the biomass from its growth medium.

The harvesting process of *Navicula* sp. TAD cells were conducted on the ninth day, when the cells reached their maximum density and exhibited optimal morphology, appearing fresh without rupturing or wrinkling, during the exponential phase of growth. Sedimentation was performed for approximately 30 minutes until the *Navicula* sp. TAD biomass settled. The relatively short sedimentation time was due to the large size and distinct shape of the cells. Filtration was carried out using nylon cloth to separate the biomass from the culture medium effectively. Biomass collected on the ninth day from a 2-liter cultivation system resulted in 4.7876 grams of wet biomass, yielding a productivity rate of 0.2659 $g{\cdot}L^{-1}{\cdot}h^{-1}$ (Figure 2c). Meanwhile, the dry biomass obtained was 1.772 grams, with a corresponding productivity of 0.098 $g{\cdot}L^{-1}{\cdot}h^{-1}$ (Figure 2d). The productivity value indicates that the cultivation system used was capable of generating a considerable amount of biomass within a relatively short period. A dry biomass productivity of 0.098 $g{\cdot}L^{-1}{\cdot}h^{-1}$ is considered efficient, especially when compared to the standard productivity range of microalgae or other microorganisms, which typically falls between 0.05–0.1 $g{\cdot}L^{-1}{\cdot}h^{-1}$ in open or semi-closed systems (Ugya and Meguellati, 2022).

3.3 Photosynthetic Pigment Extract in *Navicula* sp. TAD Cells

The crude pigment extract of *Navicula* sp. TAD was prepared by dissolving dry biomass in pure acetone solvent. According to (Hu et al., 2021), chlorophyllase enzyme activity can be inhibited using pure acetone as a solvent for photosynthetic pigments. Chlorophyllase is responsible for breaking down chlorophyll into chlorophyllide, ensuring that enzymatic activity does not degrade the chlorophyll molecules. Since the thylakoid membrane contains photosynthetic pigments, the cell disruption of *Navicula* sp. TAD is necessary for efficient extraction of pigments. Mechanical cell disruption was carried out by grinding the biomass with a mortar and pestle, followed by extraction using the maceration method for five hours in an ice bath. The resulting pigment extract exhibited a combination of carotenoid and chlorophyll pigments, visible as a light yellow-green coloration (Figure 3a). The use of an ice bath was intended to maintain pigment stability by keeping the temperature low and preventing degradation of the crude extract, as high temperatures and exposure to light can reduce pigment stability. The photosynthetic pigment extraction yielded a final extraction efficiency of 11.764%

The crude pigment extract of *Navicula* sp. TAD was identified using thin-layer chromatography (TLC). Figure 3b presents 11 spots on the chromatogram of the crude pigment extract, with corresponding Rf values. The chromatogram of the photosynthetic pigment extract from *Navicula* sp. strain TAD shows an Rf value of 0.11, belonging to the chlorophyll group (chlorophyll c). Rf values of 0.25, 0.34, 0.39, and 0.45 correspond to the carotenoid group (xanthophylls), while Rf values of 0.50, 0.54, 0.56, 0.60, and 0.64 are categorized within the chlorophyll group (chlorophyll a). An Rf value of 0.99 is associated with the carotene group (β-carotene).

3.4 Isolation of Frustules from *Navicula* sp. Strain TAD Biodiesel Waste

The isolation of frustules from *Navicula* sp. TAD frustule waste was carried out through acid washing and thermal treatment. The frustule waste is a byproduct of biomass exploration for biodiesel production, leaving behind residual diatom frustules. To remove organic and inorganic impurities soluble in acid, the frustule waste was washed with a 20% hydrochloric acid (HCl) solution. Any remaining contaminants after acid washing were eliminated by subjecting the frustules to combustion at temperatures below 600°C (Telussa et al., 2022).

The color differences in biomass samples, frustule waste, and purified *Navicula* sp. TAD frustules are shown in Figure 5. Before treatment, the *Navicula* sp. TAD biomass appeared green (Figure 4a), whereas the frustule waste exhibited a lighter green color (Figure 4b). This indicates the presence of organic residues in the frustule waste, which needed to be removed before use in electrode fabrication. After acid washing and thermal treatment, the sample appeared noticeably whiter (Figure 4c), confirming the removal of organic residues and the successful isolation of purified frustules

3.5 Morphology of *Navicula* sp. TAD Frustule

SEM Images of Diatom Biomass and Frustules Scanning Electron Microscopy (SEM) images of diatom biomass and frustules (biodiesel waste treated with 20% HCl and subjected to

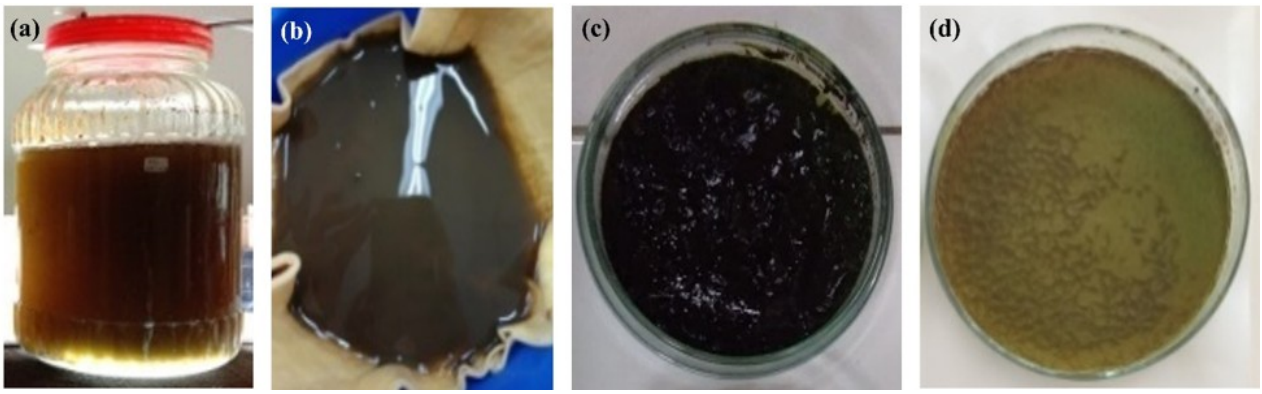

Figure 2. Biomass Harvesting of *Navicula* sp. TAD. (a) Sedimentation (b) Filtration, (c) Wet Biomass, (d) Dry Biomass

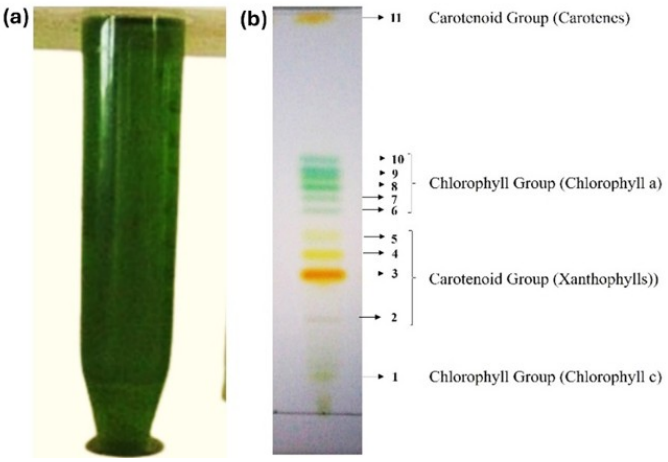

Figure 3. (a) Crude Pigment Extract of *Navicula* sp. TAD, (b) Chromatogram of the Crude Extract

combustion at 600°C) are presented in Figure 5. The surface of untreated *Navicula* sp. strain TAD biomass exhibits a non-porous structure (Figure 5a).

Meanwhile, the isolated frustules from biodiesel waste after lipid extraction exhibit a distinct micro-porous surface, clearly visible under microscopy, confirming the decomposition of surface contaminants (Figure 5b). The study findings indicate that the acid-washing treatment, followed by combustion at 600°C, effectively removes impurities while preserving the integrity of the frustule structure.

3.6 Analysis of Functional Groups in *Navicula* sp. TAD Frustule Using FTIR

Infrared radiation measurements (400–4000 cm^{-1}) were utilized to determine functional groups within molecules. The radiation absorbed by the sample is converted into molecular vibration energy, which depends on the strength and vibrational modes (stretching or bending) of the bonds. Functional group analysis using Fourier Transform Infrared Spectroscopy (FTIR) revealed characteristic peaks corresponding to the biomass and frustules of *Navicula* sp. TAD (Figure 6). The observed spectral differences indicate variations in properties and structures between the biomass and diatom frustules of *Navicula* sp. TAD, influencing its potential application as a working electrode in Dye-Sensitized Solar Cells (DSSC).

Functional group analysis using FTIR revealed characteristic peaks corresponding to the biomass and frustules of *Navicula* sp. TAD. The chemical groups identified in the *Navicula* sp. biomass included stretching vibrations of Si−O−Si at 470 cm^{-1}, bending vibrations of Si−O−Si at 1040–1095 cm^{-1}, and OH bending within hydroxyl groups at 3435 cm^{-1}. Additionally, the presence of -COOH was detected at 1734–1887 cm^{-1}, −COO at 1400–1651 cm^{-1}, and −OH from −COOH at 2523 cm^{-1}. Other functional groups included $-SO^-$ at 1231 cm^{-1}, $-R_3C-OH$ at 1072 cm^{-1}, and alkyl groups ($-CH_2^-$, $-CH_3^-$, $-CH_4^-$) at 2850–2949 cm^{-1} (Telussa et al., 2022).

For the frustules, the identified functional groups included stretching vibrations of Si−O−Si at 470 cm^{-1}, additional Si−O−Si peaks at 797–800 cm^{-1}, and bending vibrations of Si−O in Si−OH groups at 950 cm^{-1}. Further stretching vibrations of Si−O−Si appeared at 1040–1095 cm^{-1}, while hydroxyl group stretching (O−H) was detected at 3435 cm^{-1}, indicating adsorbed water and Si−O−H stretching. Peaks at 1630–1640 cm^{-1} and 3740–3780 cm^{-1} corresponded to Si−OH bonds. Compared to *Navicula* sp. biomass, frustules subjected to 20% HCl washing and combustion showed the removal of functional groups including −COOH, $-COO^-$, −OH from −COOH, $-SO^-$, $-R_3C-OH$, N−H, C=O, C−H, and C−N. This confirmed the successful purification of frustules through acid washing and combustion.

3.7 X-Ray Diffraction (XRD) Analysis

X-ray diffraction spectroscopy is a key technique for material characterization. By determining lattice structure characteristics and obtaining the nanoparticle crystal size, this method can be used to identify the crystalline phases of a material. Compared to *Navicula* sp. TAD biomass, frustules subjected to 20% HCl washing and combustion at 600°C, show the effective removal of most organic functional groups. The X-ray

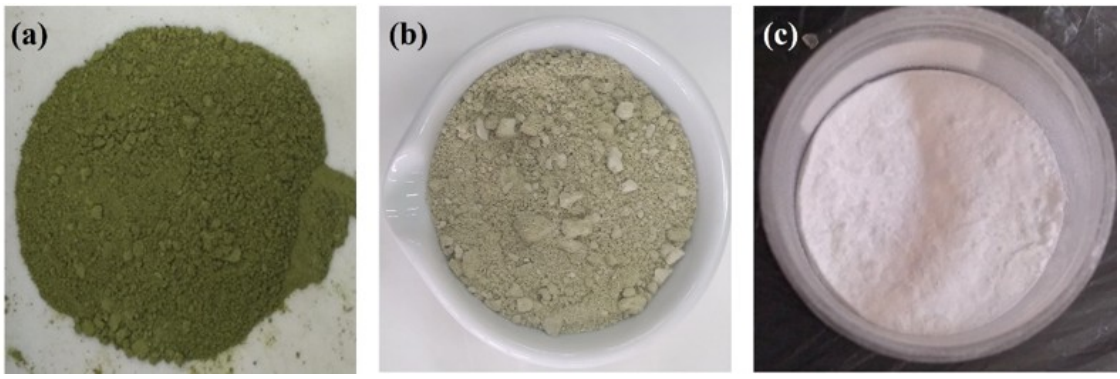

Figure 4. *Navicula* sp. TAD Samples (a) Biomass, (b) Frustule Waste, (c) Frustules After Acid Washing and Combustion at 600°C

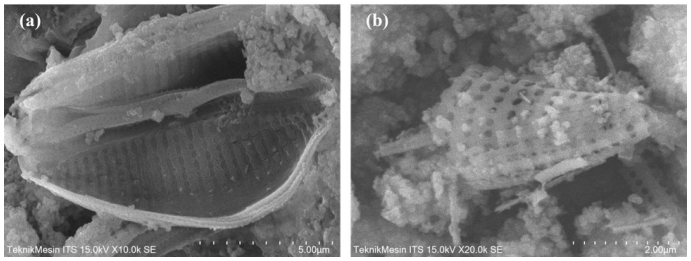

Figure 5. Morphology of *Navicula* sp. TAD (a) Biomass, (b) Frustules

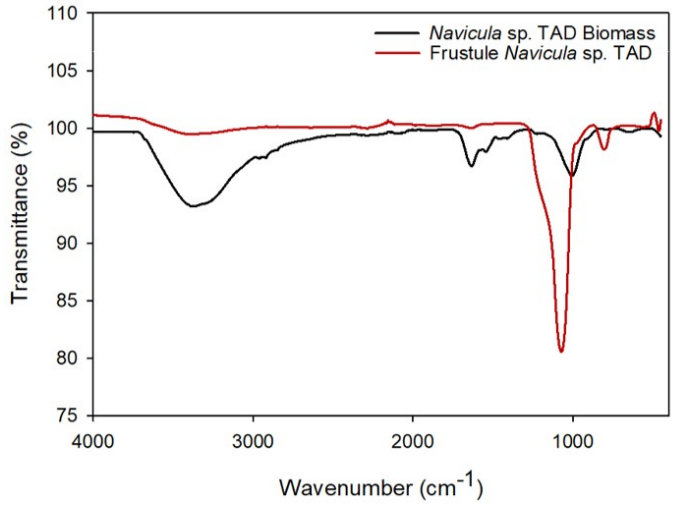

Figure 6. FTIR Spectrum of Biomass and Frustules of *Navicula* sp. TAD

diffraction pattern of frustules from *Navicula* sp. TAD waste is presented in Figure 7, exhibiting a broad reflection centered at 2θ = 20°–25°, characteristic of amorphous silica, without distinct peaks. This confirms the absence of crystalline phase peaks in the sample.

The X-ray diffraction pattern of *Navicula* sp. TAD frustules are presented in Figure 11. The diffractogram curve of *Navicula*

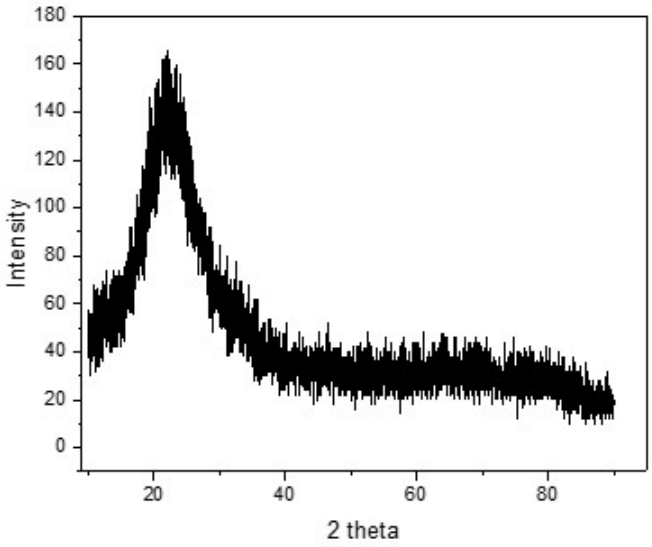

Figure 7. X-Ray Diffraction Pattern of *Navicula* sp. TAD Frustule

sp. TAD frustules exhibit a broad profile with a peak at 2θ = 21.4927°, indicating that the frustules primarily consist of SiO_2 and possess an amorphous solid structure. A similar observation was reported by Zuluaga-Astudillo et al. (2025), who conducted a characterization of diatom frustules using X-ray diffraction (XRD) analysis.

3.8 Dye-Sensitized Solar Cells Using Photosynthetic Pigments from *Navicula* sp. TAD

The fabrication of dye-sensitized solar cells (DSSCs) consists of several key components: the photoanode, cathode, electrolyte solution, and sensitizing material, which in this case is a pigment extract. DSSCs function based on the same principle as photosynthesis, where the pigment acts as a light harvester that generates excited electrons, similar to Photosystem I and II. Nanoparticles within the TiO_2 paste serve as $NADP^+$ analogs, capturing and reducing electrons. Meanwhile, the iodide/triiodide (I^-/I_3^-) electrolyte solution substitutes H_2O as the electron

donor in oxidation reactions. In this study, the pigment used as a sensitizer for the DSSC was the crude extract of photosynthetic pigments from *Navicula* sp. TAD. The paste serving as a semiconductor in the photoanode was formulated by mixing TiO_2 powder with diatom frustules from *Navicula* sp. and 96% ethanol. The photoanode, coated with either TiO_2 or a TiO_2-frustule blend (60:40 and 20:80 % w/w), was then impregnated with the pigment extract, resulting in a noticeable color change-indicating successful pigment adsorption onto the TiO_2 or TiO_2-frustule surface. The assembled photoanode was then integrated with an ITO glass substrate coated with carbon, functioning as the cathode. The electrolyte solution used in the system consisted of KI/I_3.

3.9 Characteristics of the Working Electrode in Solar Cells

3.9.1 Morphology of the Working Electrode

The nanoporous structure of the working electrode layer plays a vital role in dye-sensitized solar cells (DSSCs), particularly in facilitating dye absorption. Higher porosity allows more dye molecules to be absorbed, thereby enhancing photon capture, improving electron transfer efficiency, and boosting overall device performance. Based on Scanning Electron Microscopy (SEM) characterization, a significant structural difference is observed between the pure TiO_2 electrode and the composite electrode made from a mixture of *Navicula* sp. TAD frustules and TiO_2. The pure TiO_2 electrode exhibits a compact surface with smaller and fewer pores (Figure 8a), while the frustule-TiO_2 composite electrode shows a more heterogeneous morphology with larger and interconnected pores (Figure 8b). The frustules act as natural templates that absorb TiO_2 particles and influence surface tension, resulting in a rougher and more porous layer. Although the composite layer may appear denser visually, its internal structure enables more efficient dye diffusion, supporting better light absorption and charge transfer. This highlights the potential of biomineral-based material engineering for developing more responsive and efficient DSSCs

Image analysis using ImageJ software revealed that the working electrode fabricated from a mixture of *Navicula* sp. strain TAD frustules and TiO_2 exhibited a pore size distribution of approximately 0.1–0.2 μm (Figure 8(b); SEM scale bar 5 μm), which was notably larger than the pore size distribution observed in the pure TiO_2-based electrode, measuring only around 0.03–0.05 μm (Figure 8(a); SEM scale bar 5 μm). This difference indicates that the incorporation of frustules into the TiO_2 matrix plays a significant role in altering and enlarging the pore structure on the electrode surface. The particle size distribution in composite materials is strongly influenced by morphology and interparticle interactions. As demonstrated by Chanda (2018), synthesized TiO_2 particles exhibit a size distribution of 6–10 nm, and particle size significantly affects the optical and dielectric properties of the material. When diatom frustules are employed as natural templates, as described by Zgłobicka et al. (2021), their complex silica microstructures can guide TiO_2 particle distribution more uniformly and generate larger interparticle voids. Moreover, Soleimani et al. (2021)

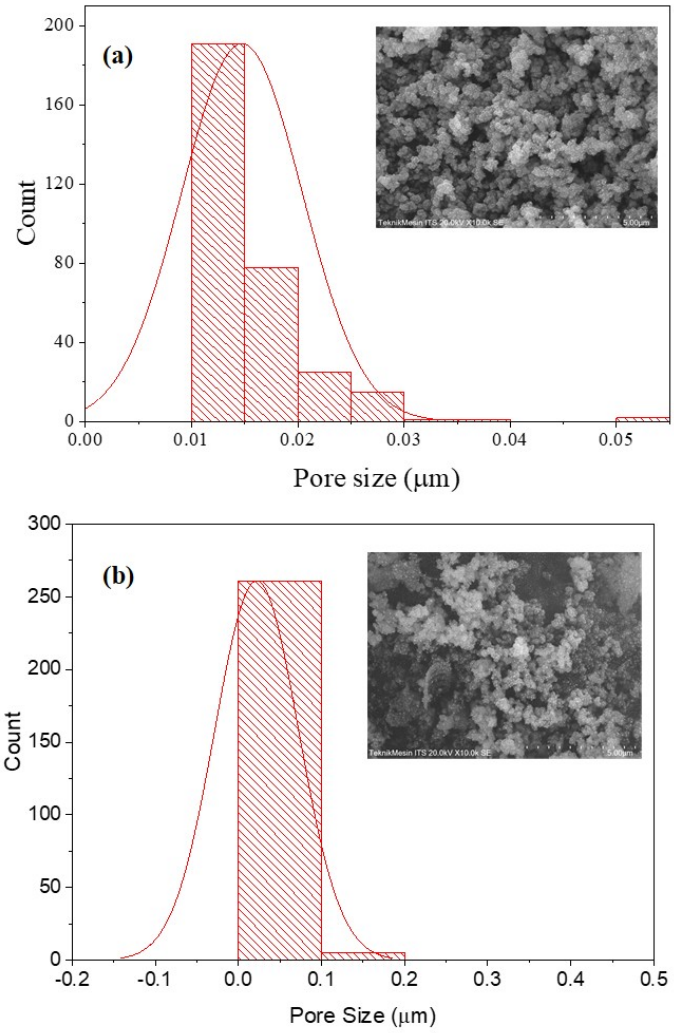

Figure 8. SEM Images and Corresponding Size Distribution Histograms of Working Electrode (a) TiO_2, (b) TiO_2-Frustule

emphasized that frustules possess high mechanical strength and intricate porous architectures, which can enhance surface roughness and overall porosity in composite electrodes.

These findings align with more recent studies that highlight the functional advantages of diatom frustules in TiO_2-based composites. Bandara et al. (2020) demonstrated that incorporating diatom frustules into TiO_2 photoelectrodes significantly enhances device performance via increased light scattering, surface area expansion, and improved charge transport. Rogato and De Tommasi (2020) further noted that frustules exhibit naturally ordered micro-/nanoporous structures capable of acting as robust scaffolds for metal oxide deposition, including TiO_2. Additionally, recent investigations into nanoparticle diffusion through diatom frustules Tomioka and Abe (2024) confirm that their hierarchical pore networks support efficient particle transport. Studies comparing frustules with synthetic silica materials also report substantially higher specific surface

area and pore volume in diatom frustules (Shady et al., 2019), reinforcing their suitability as bio-derived templates in composite electrodes. Therefore, the increased pore diameter observed in the frustule–TiO_2 composite electrode can be attributed to the redistribution and spatial organization of TiO_2 particles around the frustules, resulting in larger pore formation and potentially enhancing ion transport efficiency in electrochemical applications.

3.9.2 Functional Group Analysis of the Working Electrode Using FTIR

Characterization using Fourier Transform Infrared Spectroscopy (FTIR) was conducted to identify the presence of functional groups in the working electrode, which was fabricated using a mixture of TiO_2 and frustules, as well as TiO_2 without frustules from *Navicula* sp. TAD. The infrared spectral analysis was performed within the wavelength range of 4000–500 cm^{-1}. The results of the functional group characterization are presented in Figure 9.

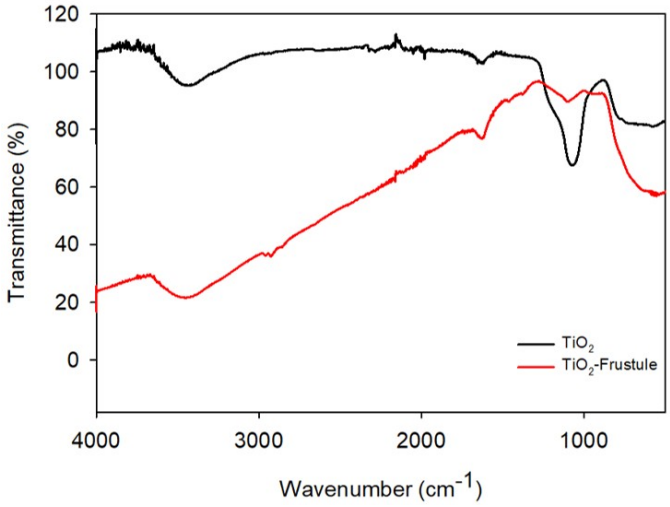

Figure 9. FTIR Spectra of the Working Electrode

Interpretation of the infrared spectra for the TiO_2 working electrode reveals characteristic vibrations with a broad absorption band of weak intensity, indicating the presence of an O−H bond at 3449.13 cm^{-1}. The absorption in the wavenumber region of 1629.41 cm^{-1} corresponds to the C−C stretching vibration, confirming the presence of carotenoid compounds. The C−O bond at 1095.99 cm^{-1}, characterized by a broad and strong absorption band, is associated with C−O stretching vibrations that represent the ether group. Additionally, Ti−O bonding is observed with a sharp absorption peak of moderate intensity at 405.67 cm^{-1}. Each absorption corresponds to the functional groups of the working electrode components, including TiO_2 paste, pigment, electrolyte solution, and carbon. In contrast, the spectrum of the TiO_2-frustule working electrode exhibits O−H bonds associated with various hydrogen-containing compounds at different intensities, with peaks at 3660, 3568, and 3435 cm^{-1}. The O−H stretching vibration from the Si−OH group absorbs strongly at 3660.01 cm^{-1}, indicating a higher intensity. Hydrogen bonding leads to the formation of broad peaks and a shift toward lower wavenumbers. At 3568.23 cm^{-1}, a sharp and intense absorption band corresponds to O−H bonding. A broad absorption peak of moderate intensity observed at 3435.45 cm^{-1} represents O−H stretching vibrations. The C−H bond at 1979.67 cm^{-1} exhibits a sharp and intense absorption band. In comparison, the wavenumber of 1617.55 cm^{-1} shows a broad and high-intensity absorption corresponding to O−H bending vibrations. The absorption at 1069.48 cm^{-1}, characterized by a broad and strong band, represents asymmetric stretching vibrations of Si−O−Si (siloxane). Additionally, at 583.68 cm^{-1}, a weak and broad absorption band is observed, while at 444.49 cm^{-1}, a weak and sharp absorption band corresponds to Ti−O−Ti stretching vibrations. Each absorption confirms the functional group characteristics of the TiO_2-frustule working electrode, the pigment, the electrolyte solution, and the carbon (Figure 9, Table 1).

Table 1. FTIR Results of TiO_2 and TiO_2-Frustule Working Electrodes of *Navicula* sp. TAD Diatoms

Functional Groups	Wavenumber (cm^{-1})	
	Working Electrodes TiO_2	Working Electrodes TiO_2-Frustule
O−H from Si−OH	-	3660.01
O−H from Si−OH	-	3568.23
O−H	3449.13	3435.45
C−H	-	1979.67
C−C	1629.41	-
Si−OH	-	1617.55
C−O	1095.99	-
Si−O−Si	-	1069.68
Ti−O	-	583.68
Ti−O	405.67	444.49

3.9.3 X-Ray Diffraction (XRD) Analysis of the Working Electrode

The X-ray diffraction (XRD) characterization curves for the TiO_2 and TiO_2-frustule working electrodes are presented in Figure 10. The diffractogram of the TiO_2 working electrode, showing characteristic peaks corresponding to the anatase phase at angles of 25.361°, 28.2039°, 35.8877°, 36.8832°, 37.7504°, 38.5327°, and 47.9753°, with the highest intensity peak observed at 2θ = 25.361°. Meanwhile, the diffractogram of the TiO_2-frustule working electrode demonstrates the formation of the anatase phase at angles of 21.6604°, 25.1692°, 35.8380°, 36.8456°, 37.6758°, 38.4681°, 42.3797°, 44.3406°, and 47.9115°, with the most intense peak at 2θ = 25.1692°.

The XRD pattern of Si-TiO_2 fundamentally exhibits a

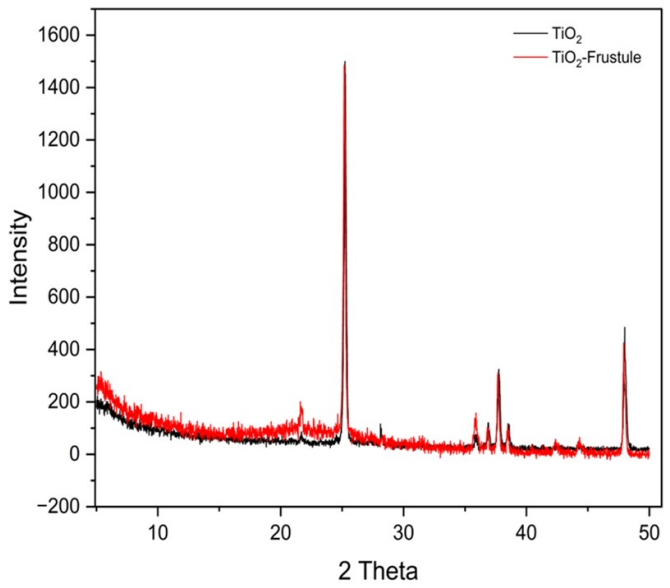

Figure 10. X-Ray Diffraction Pattern of the Working Electrode (a) TiO_2, (b) TiO_2-Frustule

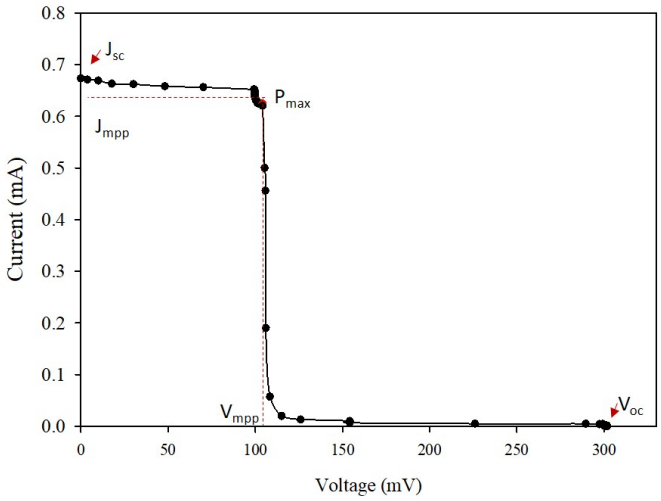

Figure 11. I-V Curve of the Solar Cell with TiO_2-Frustule Working Electrode (40:60%)

crystalline structure, as indicated by the broad characteristic diffraction peaks within the 2θ range of 20–80°. These results align with previous findings reported by Tobaldi et al. (2010), which demonstrate that the absence of Si does not alter the crystal structure of TiO_2. Consequently, the XRD spectra of Si-doped TiO_2 frustules appear nearly identical. The optical, material, and mechanical properties of diatoms make them a naturally available nanomaterial.

3.10 Measurement of Solar Cell Efficiency

Dye-sensitized solar cells (DSSCs) were evaluated for their photoelectric performance using a solar simulator. Measurements of current, voltage, and efficiency were conducted to determine the performance of each DSSC configuration, as shown in Table 2. The working electrode concentrations of TiO_2-frustule at 100:0, 40:60, and 20:80 % (w/w) yielded solar cell efficiencies of 5.06%, 10.51%, and 1.3399%, respectively. Figure 9 presents the photovoltaic curve of the solar cell sensitized with crude pigment extract from *Navicula* sp. TAD, using a TiO_2-frustule working electrode with a concentration of 40:60 % (w/w). This solar cell achieved an efficiency of 10.51%, with a short-circuit current density (Jsc) of 6.73×10^{-5} A, an open-circuit voltage (Voc) of 0.3018 V, and a fill factor (FF) of 0.32

From Figure 11 and Table 2, it is evident that the use of TiO_2 as the working electrode can achieve relatively good efficiency. This is due to its high surface roughness and porous structure, which provide a large surface area for light absorption. Dye molecules bound to the TiO_2 surface absorb incoming light, converting it into electrons. Once injected into the TiO_2, these electrons enable the generation of an electric current. The addition of frustules affects the performance of dye-sensitized solar cells (DSSC), as observed in the variations in current, voltage, and efficiency. The incorporation of frustules is expected to enhance the effective surface area of the photoelectrode compared to photoelectrodes composed solely of TiO_2. This is attributed to the relatively larger size and highly porous nanostructure of frustules. The efficiency of the solar cell using a TiO_2-frustule working electrode (60:40 % w/w) increased by 5.45% compared to the solar cell using only TiO_2 as the working electrode. This improvement can be linked to enhanced optical scattering and light trapping within the electrode. When light interacts with frustules, their porous structure induces reflections that increase the likelihood of dye molecules absorbing photons, thereby enhancing electron injection into the semiconductor and ultimately improving solar cell efficiency.

A decline in solar cell efficiency, from 10.51% to 1.3399%, was observed when the frustule concentration was increased in the TiO_2-frustule working electrode (20:80%). A higher frustule concentration enhances dye absorption, leading to greater photon absorption. However, excessive photon absorption contributes more to heat generation than electric current production. This aligns with findings by Goessling et al. (2018), which stated that an optimal frustule concentration allows frustules to function as effective light scatterers, improving light collection due to their higher refractive index compared to the surrounding media. While frustule incorporation can improve solar cell efficiency, excessive amounts may hinder electron pathway formation within the semiconductor, consequently reducing efficiency. Research on TiO_2-frustule utilization as a working electrode in solar cells has been conducted by Huang et al. (2015), who reported that solar cells fabricated with TiO_2 as the working electrode achieved an efficiency of 0.48%, with J_{sc} = 1.04 mA, V_{oc} = 0.67 V, and FF = 0.67. In contrast, solar cells using a TiO_2-frustule electrode attained an efficiency of

Table 2. Photoelectrode Characteristics of Solar Cells Using TiO_2-Frustule Derived from *Navicula* sp. TAD

Pigment Type	Working Electrode Concentration (TiO_2 : Frustule) %		
	100 : 0	40 : 60	20 : 80
Crude Extract	V_{oc} = 0.683 V J_{sc} = 4.1×10^{-4} A FF = 0.11 η = 5.06 %	V_{oc} = 0.3018 V J_{sc} = 6.73×10^{-5} A FF = 0.32 η = 10.51 %	V_{oc} = 0.234 V J_{sc} = 9.19×10^{-5} A FF = 0.39 η = 1.3399 %

3.07%, with J_{sc} = 5.70 mA, V_{oc} = 0.78 V, and FF = 0.69. This study demonstrates that incorporating frustules from *Navicula* sp. strain TAD at an appropriate concentration enhances their ability to absorb photons, resulting in increased electron generation and improved solar cell efficiency.

4. CONCLUSIONS

The efficiency of solar cells utilizing frustule waste from *Navicula* sp. TAD as a photoelectrode material demonstrated optimal photoelectric characteristics in the TiO_2:frustule 40:60% working electrode. The recorded values include J_{sc} = 0.673 mA, V_{oc} = 301.8 mV, FF = 0.32, and η = 10.51%. These results indicate that diatom frustule waste from the marine microalga *Navicula* sp. strain TAD can be employed as a working electrode to enhance dye absorption, thereby facilitating electricity generation within the solar cell.

5. ACKNOWLEDGMENT

The author expresses sincere gratitude to the dedicated staff of the Solar Cell Laboratory, Mechanical Engineering Department, Ambon State Polytechnic, for their invaluable assistance throughout the research process. Their support and expertise have significantly contributed to the successful completion of this study. Additionally, the author extends appreciation to the researchers and scholars whose published works have served as essential references in the development of this paper. Their contributions to the field have provided valuable insights that enriched the study's foundation.

REFERENCES

Baig, A., M. Siddique, and S. Panchal (2025). A Review of Visible-Light-Active Zinc Oxide Photocatalysts for Environmental Application. *Catalysts*, **15**(2); 1–26

Bandara, T. M. W. J., M. Furlani, I. Albinsson, A. Wulff, and B. E. Mellander (2020). Diatom Frustules Enhancing the Efficiency of Gel Polymer Electrolyte Based Dye-Sensitized Solar Cells with Multilayer Photoelectrodes. *Nanoscale Advances*, **2**(1); 199–209

Bhardwaj, R., A. Yadav, P. Swapnil, and M. Meena (2025). Characterization of Microalgal Beta-Carotene and Astaxanthin: Exploring Their Health-Promoting Properties Under the Effect of Salinity and Light Intensity. *Biotechnology for Biofuels and Bioproducts*, **18**(18); 1–21

Chanda, A. (2018). Structural and Magnetic Study of Undoped and Cobalt Doped TiO_2 Nanoparticles. *RSC Advances*, **8**; 10939–10947

Chen, X., C. Wang, E. Baker, and C. Sun (2015). Numerical and Experimental Investigation of Light Trapping Effect of Nanostructured Diatom Frustules. *Scientific Reports*, **5**; 11977

Chiba, Y., A. Islam, Y. Watanabe, R. Komiya, N. Koide, and L. Han (2006). Dye-Sensitized Solar Cells with Conversion Efficiency of 11.1*Japanese Journal of Applied Physics*, **45**(24–28); L638–L640

De Tommasi, E., J. Gielis, and A. Rogato (2017). Diatom Frustule Morphogenesis and Function: A Multidisciplinary Survey. *Marine Genomics*, **35**; 1–18

Dragonetti, C. and A. Colombo (2021). Recent Advances in Solar Cells. *Molecules*, **26**; 2461

Goessling, J. W., Y. Su, P. Cartaxana, C. Maibohm, L. F. Rickelt, E. C. L. Trampe, S. L. Walby, D. Wangpraseurt, X. Wu, M. Ellegaard, and M. Kühl (2018). Structure-Based Optics of Centric Diatom Frustules: Modulation of the In Vivo Light Field for Efficient Diatom Photosynthesis. *New Phytologist*, **219**(1); 122–134

Grätzel, M. (2003). Dye-Sensitized Solar Cells. *Journal of Photochemistry and Photobiology C: Photochemistry Reviews*, **4**(2); 145–153

Hara, K. and H. Arakawa (2003). Dye-Sensitized Solar Cells. In *Handbook of Photovoltaic Science and Engineering*. pages 642–674

Hu, X., I. Khan, Q. Jiao, A. Zada, and T. Jia (2021). Chlorophyllase, a Common Plant Hydrolase Enzyme with a Long History, Is Still a Puzzle. *Genes*, **12**; 1871

Huang, D. R., Y. J. Jiang, R. L. Liou, C. H. Chen, Y. A. Chen, and C. H. Tsai (2015). Enhancing the Efficiency of Dye-Sensitized Solar Cells by Adding Diatom Frustules into TiO2 Working Electrodes. *Applied Surface Science*, **347**; 64–72

Kurniawan, M. R. H., S. A. Cahyani, N. Kusumawati, P. Setiarso, and S. Muslim (2025). Optimization of Radiation and Electric Current Storage in a Dye-Sensitized Solar-Cell System Based FTO/TiO2/Acy/PVDF/C/FTO Modules for Electrical Equipment Applications. *Science and Technology Indonesia*, **10**(2); 574–587

Langer, J., J. Quist, and K. Blok (2021). Review of Renewable Energy Potentials in Indonesia and Their Contribution to a 100*Energies*, **14**(21); 7033

Latunussa, C. E. L., F. Ardente, G. Andrea, and L. Mancini (2016). Life Cycle Assessment of an Innovative Recycling Process for Crystalline Silicon Photovoltaic Panels. *Solar Energy Materials and Solar Cells*; 1–11

Müller, A., L. Friedrich, C. Reichel, S. Herceg, M. Mittag, and D. H. Neuhaus (2021). A Comparative Life Cycle Assessment of Silicon PV Modules: Impact of Module Design, Manufacturing Location and Inventory. *Solar Energy Materials and Solar Cells*, **230**; 111277

Rogato, A. and E. De Tommasi (2020). Physical, Chemical, and Genetic Techniques for Diatom Frustule Modification: Applications in Nanotechnology. *Applied Sciences*, **10**(23); 1–23

Sambrano, J. R., L. A. Vasconcellos, J. B. L. Martins, M. R. C. Santos, E. Longo, and A. Beltran (2003). A Theoretical Analysis on Electronic Structure of the (110) Surface of TiO_2-SnO_2 Mixed Oxide. *Journal of Molecular Structure: THEOCHEM*, **629**(1–3); 307–314

Shady, A. M. A., A. A. Zalat, E. A. Al-Ashkar, and M. Mohamed (2019). Nanoporous Silica of Some Egyptian Diatom Frustules as a Promising Natural Material. *Nanoscience & Nanotechnology-Asia*, **9**; 1–16

Soleimani, M., L. C. A. Van Breemen, S. P. Maddala, R. R. M. Joosten, H. Wu, I. Schreur-Piet, R. A. T. M. Van Benthem, and H. Friedrich (2021). In Situ Manipulation and Micromechanical Characterization of Diatom Frustule Constituents Using Focused Ion Beam Scanning Electron Microscopy. *Small Methods*, **5**; 2100638

Telussa, I., N. Hattu, and A. Sahalessy (2021). Morphological Observation, Identification and Isolation of Tropical Marine Microalgae from Ambon Bay, Maluku. *Indonesian Journal of Chemical Research*, **9**(2); 129–136

Telussa, I., Rahayu, and E. R. M. A. P. Lilipaly (2022). Isolation and Characterization of Biosilica as Bionanomaterial from the Waste of Frustules Diatom *Navicula* sp. TAD. *Rasayan Journal of Chemistry*; 198–203

Telussa, I., Rusnadi, and Z. Nurachman (2019). Dynamics of Beta-Carotene and Fucoxanthin of Tropical Marine *Navicula* sp. as a Response to Light Stress Conditions. *Algal Research*, **41**; 101530

Tobaldi, D. M., A. Tucci, A. S. Škapin, and L. Esposito (2010). Effects of SiO_2 Addition on TiO_2 Crystal Structure and Photocatalytic Activity. *Journal of the European Ceramic Society*, **30**(12); 2481–2490

Tomioka, N. and Y. Abe (2024). Diffusion of Individual Nanoparticles in Cylindrical Diatom Frustule. *Nanoscale Advances*; 1–6

Toster, J., K. S. Iyer, W. Xiang, F. Rosei, L. Spiccia, and C. L. Raston (2013). Diatom Frustules as Light Traps Enhance DSSC Efficiency. *Nanoscale*, **5**(3); 873–876

Ugya, A. Y. and K. Meguellati (2022). Microalgae Biomass Modelling and Optimisation for Sustainable Biotechnology: A Concise Review. *Journal of Ecological Engineering*, **23**(9); 309–318

Wahyudi, H., U. Ciptawaty, A. Ratih, and A. D. Pratama (2023). Comparison of Renewable and Non-Renewable Energy in the Long and Short Term of Indonesia Economy. *International Journal of Energy Economics and Policy*, **13**(5); 194–201

Wang, J. K. and M. Seibert (2017). Prospects for Commercial Production of Diatoms. *Biotechnology for Biofuels*, **10**(1); 1–14

Zgłobicka, I., J. Gluch, Z. Liao, S. Werner, P. Guttmann, Q. Li, P. Bazarnik, T. Plocinski, A. Witkowski, and K. J. Kurzydlowski (2021). Insight into Diatom Frustule Structures Using Various Imaging Techniques. *Scientific Reports*, **11**; 1–10

Zuluaga-Astudillo, D., J. C. Ruge, and B. Caicedo-Hormaza (2025). Micromechanical Characterization of Diatom Frustules of Multiple Origin. *Applied Sciences*, **15**(2); 5–24

